

Rapid Heating Induced Vibration of Magnetostrictive Functionally Graded Material Cylindrical Shells with Transverse Shear Effects

C.C. Hong

Department of Mechanical Engineering, Hsiuping University of Science and Technology

No. 11, Gongye Rd., Dali Dist., Taichung, 412-80 Taiwan, ROC

cchong@mail.hust.edu.tw

Abstract

The transverse shear deformation effect on the magnetostrictive functionally graded material (FGM) circular cylindrical shells under thermal vibration of rapid heating is computed by using the generalized differential quadrature (GDQ) approach. The linear, first-order shear deformation theory (FSDT) is used in the time dependent of displacement field. The dynamic equilibrium differential equations in terms of displacements and shear rotations under thermal load of rapid heating are normalized into the dynamic discrete equations. The constant value for the shear correction coefficient is simply assumed and used. The computational rapid heating solutions for thermal stresses and center deflections of circular cylindrical magnetostrictive FGM shells with four edges in simply supported boundary conditions are investigated. Some parametric effects on the FGM shells are also investigated, there are: thickness of magnetostrictive layer, control gain values, temperature of environment, power law index of FGM shells and applied heat flux.

Key Word and Phrases

Shear Deformation, FGM, Magnetostrictive, Rapid Heating, GDQ.

1. Introduction

There are some researchers describing and investigating the detail analyses of rapid heating in mold structure, steam injection and cylindrical shell. In 2012, Livshits and Kribus [1] presented a thermodynamic analysis of the solar heat hybrid steam injection gas turbine for the power plants. Simpler and less expensive solar concentrating collectors are used to provide the higher efficiency. In 2011, Li et al. [2] used the finite element method (FEM) to find the simulation solutions of large thermal stress and deformation in rapid electric heating injection mold for a large liquid crystal display (LCD) TV panel. There are some excellent LCD TV panel products can be produced with no weld marks, flow marks and other surface defects. In 2007, Bahtui and Eslami [3] obtained the FEM numerical solutions of FGM cylindrical shells under the thermal shock load. The non-linear, second-order shear deformation shell theory are considered in the equations of transverse shear strains and rotations. There are some advanced dynamic researches on the analysis and computation of composite shells. In 2013, Ponnusamy and Selvamani [4] presented the numerical computation of phase velocity for transversely isotropic magneto thermo elastic cylindrical panel by using the linear theory of thermo elasticity. In 2010, Qatu et al. [5] reviewed the articles of dynamic behaviors and results on laminated composite shells in the period of 2000-2009. Including the theories of classical, shear deformation and non-linear are presented. In 2006, Lee et al. [6] investigated the transverse deflection damping analysis on laminated composite shells with Terfenol-D material by using the FEM computation with a non-linear, third-order shear deformation theory. In 2005, Jafari et al. [7] studied the free and forced transient dynamic vibrations of composite circular cylindrical shells included the effect of linear, first-order shear deformation shell theory.

The author has some generalized differential quadrature (GDQ) experiences in the thermal vibration study of Terfenol-D FGM shells and plates. In 2014, Hong [8] studied the thermal vibration and transient response of Terfenol-D FGM plates by considering the effects of modified shear correction coefficient values. In 2013, Hong [9] studied the thermal vibration of Terfenol-D FGM shells without considering the effects of transverse shear deformation. In 2010, Hong [10] presented the computational approach of piezoelectric shells by considering the effects of first-

order transverse shear deformation. It is interesting to obtain the rapid heating GDQ results of thermal stresses and center deflections under uncontrolled/controlled gain by considering the linear, first-order transverse shear deformation effect on magnetostrictive FGM shells. Some parametric effects on the rapid heating of FGM shells are also investigated, there are: thickness of magnetostrictive layer, control gain values, temperature of environment, power-law index of FGM and applied heat flux.

2. Formulation

2.1 Properties of FGM

For a two-material FGM circular cylindrical shell under rapid heating as shown in (Fig.1), where z is the thickness coordinate, h is the thickness of FGMs shell. The material properties for Young's module of non-linear power-law function in two-material FGM circular cylindrical shell can be expressed as follows by Chi and Chung in 2006 [11].

$$E_{fgm} = (E_2 - E_1) \left(\frac{z + h/2}{h} \right)^{R_n} + E_1 \quad (2.1)$$

and the others $\nu_{fgm}, \rho_{fgm}, \alpha_{fgm}, \kappa_{fgm}, C_{vfgm}$ are assumed in the simple average form, this choice of assumption is quite reasonable for the Young's module is in the main and greater value (GPa unit) of properties than the others, and the motivation for the using of simple average properties form is for the direct stiffness integration can be in the more simply calculation, where R_n is the power law index, E_{fgm} is the Young's module, ν_{fgm} is the Poisson's ratio, ρ_{fgm} is the density, α_{fgm} is the thermal expansion coefficient, κ_{fgm} is the thermal conductivity, C_{vfgm} is the specific heat of the FGM shell. The terms of Young's modulus E_1, E_2 are the constituent material 1 and material 2, respectively are expressed corresponding to the non-linear individual constituent material properties term P_i , in which $P_i = P_0(P_{-1}T^{-1} + 1 + P_1T + P_2T^2 + P_3T^3)$ are in functions of temperature coefficient parameters $P_0, P_{-1}, P_1, P_2, P_3$ and environment temperature T .

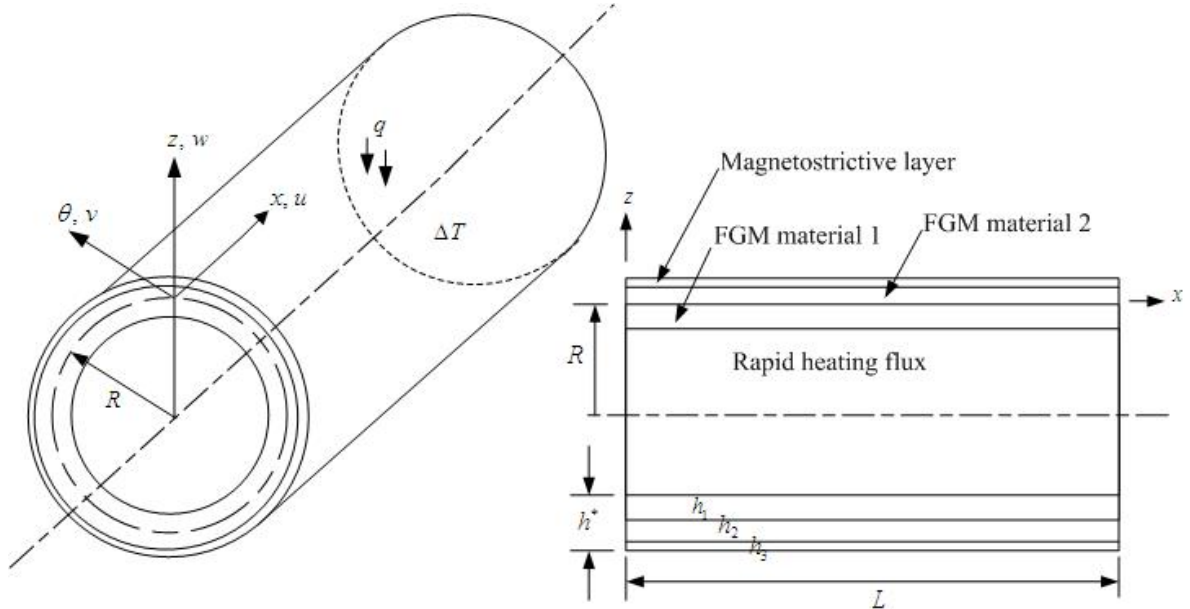


Fig. 1 Magnetostrictive FGM circular cylindrical shell under rapid heating .

2.2 Displacement Field

The displacements u, v and w of circular cylindrical magnetostrictive FGM shells are assumed in the first-order shear deformation theory (FSDT) model by Qatu et al. in 2010 [5] as follows.

$$\begin{aligned} u &= u_0(x, \theta, t) + z\phi_x(x, \theta, t) \\ v &= v_0(x, \theta, t) + z\phi_\theta(x, \theta, t) \\ w &= w(x, \theta, t) \end{aligned} \quad (2.2)$$

where u_0 , v_0 are tangential displacements. w is transverse displacement of the middle-surface of the shell. ϕ_x , ϕ_θ are middle-surface shear rotations. x , θ are in-surface coordinates of the shell. z is out of surface coordinate of the shell. t is time. The use of FSDT model for such a shell problem is a big limitation for obtaining the linear, simple, preliminary and basic calculations of strains, stresses and equations of motion. Similarly thick shell problems in the literature are further investigated with non-linear, refined and higher order models to get more accurate results.

2.3 GDQ Method

Shu and Richards presented the GDQ method in 1990 and can be stated in the referred papers by Hong in 2014 [8], by Bert et al. in 1989 [12], by Shu and Du in 1997 [13]. The GDQ method approximates the derivative of function is used in the formulation.

2.4 Thermo-elastic Stress-Strain Relations with Magnetostrictive Effect

The circular cylindrical FGM shell mounted with magnetostrictive layers under rapid heating, which is shown in (Fig.1), where L is the axial length of shell, h^* is the total thickness of magnetostrictive layer and FGM shell, h_3 is the thickness of magnetostrictive layer, h_1 and h_2 are the thickness of FGM material 1 and FGM material 2, respectively, $\Delta T = T_{0rapid}(x, \theta, t) + \frac{z}{h^*}T_1(x, \theta, t)$ is the temperature difference between the FGM shell and a reference state, T_{0rapid} is the temperature rise due to the rapid heating flux starts acting over inner surface of FGM shells, T_1 is the general temperature parameter.

For the plane stresses in the FGM circular cylindrical shell, the in-plane stresses constitute the membrane stresses, bending stresses and thermal stresses with magnetostrictive effect for the k^{th} layer are in the following equations by Hong in 2014 [8], by Lee and Reddy in 2005 [14].

$$\begin{Bmatrix} \sigma_x \\ \sigma_\theta \\ \sigma_{x\theta} \end{Bmatrix}_{(k)} = \begin{bmatrix} \bar{Q}_{11} & \bar{Q}_{12} & \bar{Q}_{16} \\ \bar{Q}_{12} & \bar{Q}_{22} & \bar{Q}_{26} \\ \bar{Q}_{16} & \bar{Q}_{26} & \bar{Q}_{66} \end{bmatrix}_{(k)} \begin{Bmatrix} \varepsilon_x - \alpha_x \Delta T \\ \varepsilon_\theta - \alpha_\theta \Delta T \\ \varepsilon_{x\theta} - \alpha_{x\theta} \Delta T \end{Bmatrix}_{(k)} - \begin{bmatrix} 0 & 0 & \tilde{e}_{31} \\ 0 & 0 & \tilde{e}_{32} \\ 0 & 0 & \tilde{e}_{36} \end{bmatrix}_{(k)} \begin{Bmatrix} 0 \\ 0 \\ \tilde{H}_z \end{Bmatrix}_{(k)} \quad (2.3a)$$

and the shear stresses are given as follows.

$$\begin{Bmatrix} \sigma_{\theta z} \\ \sigma_{xz} \end{Bmatrix}_{(k)} = \begin{bmatrix} \bar{Q}_{44} & \bar{Q}_{45} \\ \bar{Q}_{45} & \bar{Q}_{55} \end{bmatrix}_{(k)} \begin{Bmatrix} \varepsilon_{\theta z} \\ \varepsilon_{xz} \end{Bmatrix}_{(k)} - \begin{bmatrix} \tilde{e}_{14} & \tilde{e}_{24} & 0 \\ \tilde{e}_{15} & \tilde{e}_{25} & 0 \end{bmatrix}_{(k)} \begin{Bmatrix} 0 \\ 0 \\ \tilde{H}_z \end{Bmatrix}_{(k)} \quad (2.3b)$$

where α_x and α_θ are the coefficients of thermal expansion. $\alpha_{x\theta}$ is the coefficient of thermal shear. \bar{Q}_{ij} is the stiffness of FGM shell. ε_x , ε_θ and $\varepsilon_{x\theta}$ are not negligible in-plane strains. $\varepsilon_{\theta z}$ and ε_{xz} are shear strains. The curvatures of k_x , k_θ and $k_{x\theta}$, respectively in terms of displacement components and shear rotation are given as follows.

$$\begin{aligned} \varepsilon_x &= \frac{\partial u_0}{\partial x} + z \frac{\partial \phi_x}{\partial x} \\ \varepsilon_\theta &= \frac{1}{R} \left(\frac{\partial v_0}{\partial \theta} + z \frac{\partial \phi_\theta}{\partial \theta} + w \right) \end{aligned}$$

$$\begin{aligned}
 \varepsilon_{x\theta} &= \frac{\partial v_0}{\partial x} + z \frac{\partial \phi_\theta}{\partial x} + \frac{1}{R} \left(\frac{\partial u_0}{\partial \theta} + z \frac{\partial \phi_x}{\partial \theta} \right) \\
 \varepsilon_{\theta z} &= \phi_\theta + \frac{1}{R} \frac{\partial w}{\partial \theta} - \frac{v_0}{R} \\
 \varepsilon_{xz} &= \phi_x + \frac{\partial w}{\partial x} - \frac{u_0}{R} \\
 k_x &= \frac{\partial \phi_x}{\partial x} \\
 k_\theta &= \frac{1}{R} \frac{\partial \phi_\theta}{\partial \theta} \\
 k_{x\theta} &= \frac{\partial \phi_\theta}{\partial x} + \frac{1}{R} \frac{\partial \phi_x}{\partial \theta}
 \end{aligned} \tag{2.4}$$

in which R is the middle-surface radius of shell. \tilde{e}_{ij} is the transformed magnetostrictive coupling modulus. \tilde{H}_z is the magnetic field intensity can be expressed as follows.

$$\tilde{H}_z(x, y, t) = k_c c(t) \frac{\partial w}{\partial t} \tag{2.5}$$

where k_c is the coil constant. $c(t)$ is the control gain. For the preliminary stresses calculation, simpler forms of \bar{Q}_{ij} for circular cylindrical FGM shells are given as follows by Qatu et al. in 2010 [5].

$$\begin{aligned}
 \bar{Q}_{11} = \bar{Q}_{22} &= \frac{E_{fgm}}{1 - \nu_{fgm}^2} \\
 \bar{Q}_{12} = \bar{Q}_{21} &= \frac{\nu_{fgm} E_{fgm}}{(1 + z/R)(1 - \nu_{fgm})} \\
 \bar{Q}_{66} &= \frac{E_{fgm}}{2(1 + z/R)(1 + \nu_{fgm})} \\
 \bar{Q}_{44} &= \frac{E_{fgm}}{2(1 + \nu_{fgm})} \\
 \bar{Q}_{55} &= \frac{E_{fgm}}{2(1 + z/R)(1 + \nu_{fgm})} \\
 \bar{Q}_{16} = \bar{Q}_{26} = \bar{Q}_{45} &= 0
 \end{aligned} \tag{2.6a}$$

The term $(1 + z/R)$ included in the reduced elastic coefficients is considered the effect of thickness with radius on E_{fgm} for the not shallow shell in the calculation of stresses. The $(1 + z/R)$ terms are usually included in the geometrical relations such those for strains given in equations (2.4), but for the attention on stiffness of FGM shell, it is chosen to place in the side of reduced elastic coefficients. For magnetostrictive layer, simple \bar{Q}_{ij} are expressed as follows.

$$\begin{aligned}
 \bar{Q}_{11} = \bar{Q}_{22} &= E_{11} \\
 \bar{Q}_{66} &= E_{11}/2 \\
 \bar{Q}_{12} = \bar{Q}_{16} = \bar{Q}_{26} &= 0
 \end{aligned} \tag{2.6b}$$

in which E_{11} is the Young's modulus for the magnetostrictive material.

2.5 Dynamic equilibrium differential equations

The dynamic equations of motion for a circular cylindrical shell introduced by Jafari et al. in 2005 [7] are given as follows.

$$\begin{aligned}
 \frac{\partial N_x}{\partial x} + \frac{1}{R} \frac{\partial N_{x\theta}}{\partial \theta} &= \rho \frac{\partial^2 u}{\partial t^2} + H \frac{\partial^2 \phi_x}{\partial t^2} \\
 \frac{\partial N_{x\theta}}{\partial x} + \frac{1}{R} \frac{\partial N_\theta}{\partial \theta} + \frac{1}{R} Q_\theta + N_a \frac{\partial^2 v}{\partial x^2} &= \rho \frac{\partial^2 v}{\partial t^2} + H \frac{\partial^2 \phi_\theta}{\partial t^2} \\
 \frac{\partial Q_x}{\partial x} + \frac{1}{R} \frac{\partial Q_\theta}{\partial \theta} - \frac{1}{R} N_\theta + N_a \frac{\partial^2 w}{\partial x^2} - q &= \rho \frac{\partial^2 w}{\partial t^2} \\
 \frac{\partial M_x}{\partial x} + \frac{1}{R} \frac{\partial M_{x\theta}}{\partial \theta} - Q_x &= H \frac{\partial^2 u}{\partial t^2} + I \frac{\partial^2 \phi_x}{\partial t^2} \\
 \frac{\partial M_{x\theta}}{\partial x} + \frac{1}{R} \frac{\partial M_\theta}{\partial \theta} - Q_\theta &= H \frac{\partial^2 v}{\partial t^2} + I \frac{\partial^2 \phi_\theta}{\partial t^2}
 \end{aligned} \tag{2.7}$$

where $(\rho, H, I) = \int_{-\frac{h^*}{2}}^{\frac{h^*}{2}} \rho_0(1, z, z^2) dz$, ρ_0 is the density of ply. N_a is the pulsating axial load. q is the applied external pressure load. N_x , N_θ , $N_{x\theta}$, M_x , M_θ , $M_{x\theta}$, Q_x and Q_θ are stress resultants.

The constitutive relations including thermal and magnetostrictive loads effect introduced by Lee et al. in 2006 [6] are given as follows.

$$\begin{aligned}
 \begin{Bmatrix} N_x \\ N_\theta \\ N_{x\theta} \\ M_x \\ M_\theta \\ M_{x\theta} \end{Bmatrix} &= \begin{bmatrix} A_{11} & A_{12} & 0 & B_{11} & B_{12} & 0 \\ A_{12} & A_{22} & 0 & B_{12} & B_{22} & 0 \\ 0 & 0 & A_{66} & 0 & 0 & B_{66} \\ B_{11} & B_{12} & 0 & D_{11} & D_{12} & 0 \\ B_{12} & B_{22} & 0 & D_{12} & D_{22} & 0 \\ 0 & 0 & B_{66} & 0 & 0 & D_{66} \end{bmatrix} \begin{Bmatrix} \varepsilon_x \\ \varepsilon_\theta \\ \varepsilon_{x\theta} \\ k_x \\ k_\theta \\ k_{x\theta} \end{Bmatrix} - \begin{Bmatrix} \bar{N}_x \\ \bar{N}_\theta \\ \bar{N}_{x\theta} \\ \bar{M}_x \\ \bar{M}_\theta \\ \bar{M}_{x\theta} \end{Bmatrix} = \begin{Bmatrix} \tilde{N}_x \\ \tilde{N}_\theta \\ \tilde{N}_{x\theta} \\ \tilde{M}_x \\ \tilde{M}_\theta \\ \tilde{M}_{x\theta} \end{Bmatrix} \\
 \begin{Bmatrix} Q_x \\ Q_\theta \end{Bmatrix} &= \begin{bmatrix} A_{55} & 0 \\ 0 & A_{44} \end{bmatrix} \begin{Bmatrix} \varepsilon_{xz} \\ \varepsilon_{\theta z} \end{Bmatrix}
 \end{aligned} \tag{2.8}$$

where:

$$\begin{aligned}
 (A_{ij}, B_{ij}, D_{ij}) &= \int_{-\frac{h^*}{2}}^{\frac{h^*}{2}} \bar{Q}_{ij}(1, z, z^2) dz \\
 A_{i^*j^*} &= \int_{-\frac{h^*}{2}}^{\frac{h^*}{2}} k_\alpha k_\beta \bar{Q}_{i^*j^*} dz, \quad (i^*, j^* = 4, 5; \alpha = 6 - i^*, \beta = 6 - j^*) \\
 (\bar{N}_x, \bar{M}_x) &= \int_{-\frac{h^*}{2}}^{\frac{h^*}{2}} (\bar{Q}_{11} \alpha_x + \bar{Q}_{12} \alpha_\theta + \bar{Q}_{16} \alpha_{x\theta}) \Delta T(1, z) dz \\
 (\bar{N}_\theta, \bar{M}_\theta) &= \int_{-\frac{h^*}{2}}^{\frac{h^*}{2}} (\bar{Q}_{12} \alpha_x + \bar{Q}_{22} \alpha_\theta + \bar{Q}_{26} \alpha_{x\theta}) \Delta T(1, z) dz \\
 (\bar{N}_{x\theta}, \bar{M}_{x\theta}) &= \int_{-\frac{h^*}{2}}^{\frac{h^*}{2}} (\bar{Q}_{16} \alpha_x + \bar{Q}_{26} \alpha_\theta + \bar{Q}_{66} \alpha_{x\theta}) \Delta T(1, z) dz
 \end{aligned}$$

$$\begin{aligned}
 (\tilde{N}_x, \tilde{M}_x) &= \int_{-\frac{h^*}{2}}^{\frac{h^*}{2}} \tilde{e}_{31} \tilde{H}_z(1, z^2) dz \\
 (\tilde{N}_\theta, \tilde{M}_\theta) &= \int_{-\frac{h^*}{2}}^{\frac{h^*}{2}} \tilde{e}_{32} \tilde{H}_z(1, z^2) dz \\
 (\tilde{N}_{x\theta}, \tilde{M}_{x\theta}) &= \int_{-\frac{h^*}{2}}^{\frac{h^*}{2}} \tilde{e}_{36} \tilde{H}_z(1, z^2) dz \\
 (N_a, M_a) &= \int_{-\frac{h^*}{2}}^{\frac{h^*}{2}} (\bar{Q}_{11} \alpha_x + \bar{Q}_{12} \alpha_\theta + \bar{Q}_{16} \alpha_{x\theta}) T_{0rapid}(1, z) dz
 \end{aligned}$$

in which k_α and k_β are the shear correction coefficients, N_a and M_a are the pulsating axial load and moment in function of T_{0rapid} . The A_{11} term can be obtained as follows.

$$A_{11} = \frac{h}{1 - \left(\frac{v_1 + v_2}{2}\right)^2} \left(\frac{R_n E_1 + E_2}{R_n + 1} \right) + E_{11} h_3. \quad (2.9)$$

The dynamic equilibrium differential equations of magnetostrictive FGM circular cylindrical shells in terms of displacements and shear rotations can be obtained.

2.6 Dynamic Discrete Equations

By using the two-dimensional GDQ method to discrete the differential equations under the following vibrations of time sinusoidal displacements, shear rotations and temperature parameter.

$$\begin{aligned}
 u &= [u_0(x, \theta) + z\phi_x(x, \theta)] \sin(\omega_{mn}t) \\
 v &= [v_0(x, \theta) + z\phi_\theta(x, \theta)] \sin(\omega_{mn}t) \\
 w &= w(x, \theta) \sin(\omega_{mn}t) \\
 \phi_x &= \phi_x(x, \theta) \sin(\omega_{mn}t) \\
 \phi_\theta &= \phi_\theta(x, \theta) \sin(\omega_{mn}t)
 \end{aligned} \quad (2.10)$$

$$\Delta T = \left(\bar{T}_{0rapid} + \frac{z}{h^*} \bar{T}_1 \right) \sin(\pi x / L) \sin(\pi \theta) \sin(\gamma t) \quad (2.11a)$$

where ω_{mn} is the natural frequency of the shell, γ is the frequency of applied heat flux, \bar{T}_1 is the amplitude of temperature.

When the magnetostrictive FGM shell begins subjected to the raping heating acting over inner surface and the non-linear, simple rapid heat temperature equation is used as follows by Hetnarski in 1987 [15], by Carslaw and Jaeger in 1959 [16].

$$\bar{T}_{0rapid} = \frac{h^* q_0}{\kappa_{fgm}} \left[\frac{\beta t}{\pi^2} + \frac{1}{2} \left(\frac{z}{h^*} + \frac{1}{2} \right)^2 - \frac{1}{6} - \frac{2}{\pi^2} \sum_{j=1}^{\infty} \frac{(-1)^j}{j^2} e^{-j^2 \beta t} \cos j\pi \left(\frac{z}{h^*} + \frac{1}{2} \right) \right] \quad (2.11b)$$

where $\beta = \pi^2 \kappa_{fgm} / h^{*2}$, q_0 is the applied heat flux.

By considering for four sides simply supported, the dynamic discrete equations in matrix notation can be obtained. And the following frequency parameter f^* can be used.

$$f^* = 4\pi\omega_{mn}R\sqrt{I/A_{11}} \quad (2.12)$$

3. Some Numerical Results and Discussions

The vibration and transient response results of rapid heating on inner surface of Terfenol-D FGM shells without considering the effects of shear deformation are already investigated in the

referred paper by Hong in 2014 [17] with the same GDQ approach. The FGM material 1 is SUS304, the FGM material 2 is Si_3N_4 used in the GDQ computations. The magnetostrictive material Terfenol-D made in USA is used and the elastic modules are listed in the referred papers by Reddy and Chin in 1998 [18], by Shariyat in 2008 [19]. Three-layer ($0^\circ / 0^\circ / 0^\circ$) circular cylindrical Terfenol-D FGM shell including shear deformation is considered. The superscript of m denotes magnetostrictive layer. The following coordinates for the grid points are used:

$$\begin{aligned} x_i &= 0.5[1 - \cos(\frac{i-1}{N-1}\pi)]L, \quad i = 1, 2, \dots, N \\ \theta_j &= 0.5[1 - \cos(\frac{j-1}{M-1}\pi)]2\pi, \quad j = 1, 2, \dots, M \end{aligned} \quad (3.1)$$

The use of the shear correction factor $5/6$ sounds as an incongruity. $5/6$ value has been calculated for known boundary conditions, loading conditions and material properties. Although it is not sure that it is also valid for the cases investigated in the present paper but for this rapid heating FGM shell firstly study might be usually used to obtain a referred data. In fact an opportune shear correction factor should be calculated for each case by Hong in 2014 [20]. To obtain the vibration frequency ω_{mn} , it is reasonable to assumed that u_0, v_0, w, ϕ_x and ϕ_θ are expressed in time sinusoidal form of free vibration for shell under four sides simply supported as follows:

$$\begin{aligned} u_0 &= a_{mn} e^{i\omega_{mn}t} \cos(m\pi x/L) \cos(n\theta) \\ v_0 &= b_{mn} e^{i\omega_{mn}t} \sin(m\pi x/L) \sin(n\theta) \\ w &= c_{mn} e^{i\omega_{mn}t} \sin(m\pi x/L) \cos(n\theta) \\ \phi_x &= d_{mn} e^{i\omega_{mn}t} \cos(m\pi x/L) \cos(n\theta) \\ \phi_\theta &= e_{mn} e^{i\omega_{mn}t} \sin(m\pi x/L) \sin(n\theta) \end{aligned} \quad (3.2)$$

Table 1 Convergence of cylindrical Terfenol-D FGM shells with $q_0 = 2 \text{ J}/(s \cdot m^2)$

L/h^*	GDQ method	Deflection $w(L/2, 2\pi/2)$ at $t = 0.1s$		
	$N \times M$	$L/R = 0.05$	$L/R = 0.1$	$L/R = 1.0$
8	15 × 15	1.62987	1.62875	0.220517
	17 × 17	1.63093	1.63178	0.223689
	19 × 19	1.63250	1.63174	0.223684
7	15 × 15	0.815342	0.705802	0.132015
	17 × 17	0.815115	0.706775	0.133330
	19 × 19	0.814998	0.706685	0.133331
5	15 × 15	0.140216	0.126730	0.354642E-01
	17 × 17	0.140170	0.126726	0.355299E-01
	19 × 19	0.140124	0.126764	0.355299E-01

where m is the number of axial half-waves, n is the number of circumferential waves, $a_{mn}, b_{mn}, c_{mn}, d_{mn}$ and e_{mn} are the amplitudes of time sinusoidal form.

Firstly, the computational rapid heating results of the amplitude of center deflection $w(L/2, 2\pi/2)$ (unit mm) dynamic convergence study in circular cylindrical Terfenol-D FGM shells are obtained and listed in Table 1 with heat flux value $q_0 = 2 \text{ J}/(s \cdot m^2)$, $k_c c(t) = 0$, $t = 0.1s$, $h^* = 1.2 \text{ mm}$, $h_3 = 1 \text{ mm}$, $h_1 = h_2 = 0.1 \text{ mm}$, $q = 0$, $m = n = 1$, $R_n = 1$,

$T = 653^\circ K$, $\bar{T}_1 = 1^\circ K$. The error accuracy of deflection $w(L/2, 2\pi/2)$ is $2.235E-05$ for $L/h^* = 8$ and $L/R = 1.0$. The 19×19 grid point is found in the acceptable, good convergence result. Secondly, Table 2 shows the suitable gain values $k_c c(t)$ versus time t for $R_n = 1$, thick shell $L/h^* = 5$ at $q_0 = 2 J/(s \cdot m^2)$ and $T = 653^\circ K$.

Table 2 $k_c c(t)$ versus t for $R_n = 1$, $q_0 = 2 J/(s \cdot m^2)$

L/h^*	$t = 0.1s \sim 0.8s$	$t = 0.9s$	$t = 1.0s \sim 1.4s$	$t = 1.5s \sim 3.0s$
	$k_c c(t)$	$k_c c(t)$	$k_c c(t)$	$k_c c(t)$
5	10^9	-10^8	-10^7	-10^8

Fig.2a shows the frequency parameter f^* versus n results investigated by using the GDQ method for the four sides simply supported circular cylindrical Terfenol-D FGM shells, $h^*/R = 0.01$, $L/R = 0.05$, stacking sequence $(0^\circ / 0^\circ / 0^\circ)$ at $t = 6s$, $T_{0,rapid} = 0$, $k_c c(t) = 0$, $R_n = 1$. Fig.2b shows the re-plotted, compared frequency parameter ω^* versus n by Jafari et al. in 2005 [7] with equation $\omega^* = \omega_{mn} L_s \sqrt{\rho h^* / A_{11}}$, in which $L_s = 2\pi R$, for the clamped-free composite cylindrical shell, $h^*/R = 0.002$, $L/R = 20$, stacking sequence $(90^\circ / 0^\circ / 90^\circ)$, Young's modulus: $E_{11} = 19GPa$, $E_{22} = 7.6GPa$. The very good tendency is obtained between the two curves of frequency parameter versus n , also frequency parameters are increasing with n values. Since the frequency parameters f^* and ω^* are obtained in the two different boundary conditions and property values, so the magnitudes of f^* and ω^* are totally different. These assessments in slopes versus n are calculated and shown in Table 3 to provide the slope values are all increasing with n .

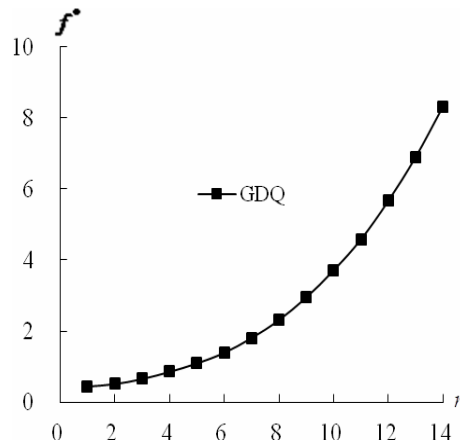


Fig. 2a f^* versus n results by the GDQ method

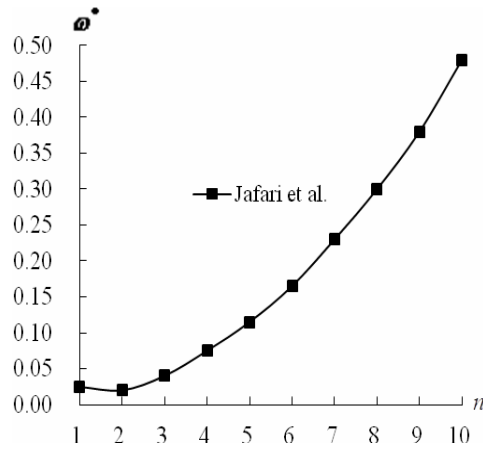


Fig. 2b Compared ω^* versus n results

Fig. 2 Frequency parameter f^* versus n and compared ω^* versus n

Table 3 Assessments in slope versus n for presented GDQ and Jafari et al. methods

Methods	$n=2$	$n=3$	$n=4$	$n=5$	$n=6$	$n=7$	$n=8$	$n=9$
	slope	slope	slope	slope	slope	slope	slope	slope
GDQ	0.11	0.17	0.22	0.27	0.36	0.46	0.57	0.70
Jafari et al.	0.01	0.03	0.04	0.05	0.06	0.07	0.08	0.09

Figs. 3 & 4 show the response values of center deflection amplitude $w(L/2, 2\pi/2)$ (unit mm) and dominated stresses σ_x (unit GP_a) at center position of outer surface $Z = 0.5h^*$, respectively versus time t under $q_0 = 2 J/(s \cdot m^2)$, for thick shell $L/h^* = 5$, $L/R = 1$, $R_n = 1$, $T = 653^\circ K$, $\bar{T}_1 = 1^\circ K$, $t = 0.1s-3.0s$, time step is 0.1s. Usually there is no limit for the time domain, figures in the rapid heating approach for $t = 0.1s-3.0s$ are provided. The controlled values of the center deflection $w(L/2, 2\pi/2)$ with $k_c(t)$ are smaller than the uncontrolled values of $w(L/2, 2\pi/2)$ without $k_c(t)$. The greatest value of center deflection is 1.79508mm occurred at $t=0.7s$ for $L/h^* = 5$. The amplitude $w(L/2, 2\pi/2)$ can be controlled and adjusted to a desired smaller value by using the suitable $k_c(t)$ value in Terfenol-D FGM shell. The Terfenol-D FGM shell under controlled gain values has the larger absolute stresses σ_x than uncontrolled gain values case at $t = 0.1s-0.6s$. The absolute values of stresses σ_x are increasing with t .

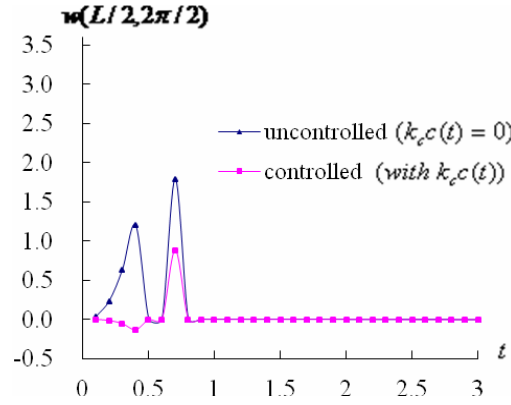


Fig. 3 $w(L/2, 2\pi/2)$ versus t for $L/h^* = 5$

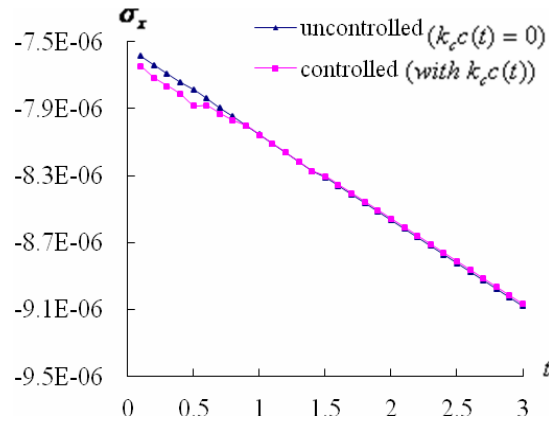


Fig. 4 σ_x versus t for $L/h^* = 5$

Figs. 5 & 6 show the center deflection amplitude $w(L/2, 2\pi/2)$ (unit mm) and dominated stress σ_x (unit GP_a) at center position of outer surface, respectively versus thickness h_3 (unit mm) of magnetostrictive layer in Terfenol-D FGM shell under rapid heating $q_0 = 2 \text{ J}/(\text{s} \cdot \text{m}^2)$ with $k_c c(t) = -10^8$ for $T = 653^\circ \text{K}$, $\bar{T}_1 = 1^\circ \text{K}$, $L/h^* = 5$, $L/R = 1.0$ at $t = 3 \text{ s}$. The absolute values of center deflection $w(L/2, 2\pi/2)$ are decreasing with h_3 from 0.36 to 0.48mm, increasing with h_3 from 0.48 to 0.72mm and decreasing with h_3 from 0.72 to 0.90mm for all different values of R_n . The absolute σ_x values are increasing with h_3 from 0.36 to 0.72mm and decreasing with h_3 from 0.72 to 0.90mm for all different values of R_n .

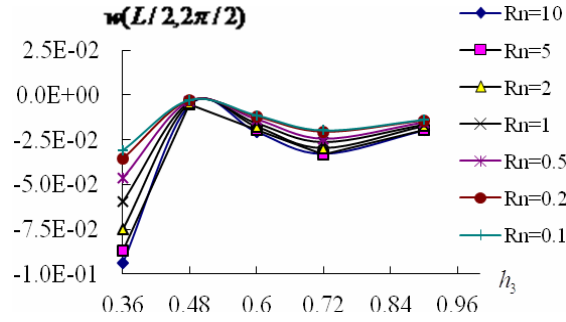


Fig. 5 $w(L/2, 2\pi/2)$ versus h_3 for $T = 653^\circ K$

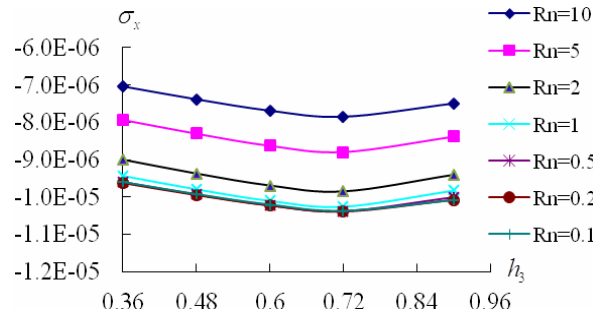


Fig. 6 σ_x versus h_3 for $T = 653^\circ K$

Figs. 7 & 8 show the center deflection amplitude $w(L/2, 2\pi/2)$ (unit mm) versus T for $q_0 = 2 J/(s \cdot m^2)$ and versus q_0 for $T = 100^\circ K$, respectively of Terfenol-D FGM shell with $k_c c(t) = 10^9$ under $\bar{T}_1 = 1^\circ K$, $L/h^* = 5$, $L/R = 1.0$ at $t = 0.1$ s. The absolute value of amplitude $w(L/2, 2\pi/2)$ can be controlled and adjusted to a desired smaller value under higher temperature $T \geq 400^\circ K$ for $R_n = 0.1$ only, for the others R_n the amplitude $w(L/2, 2\pi/2)$ are little increasing with T . The center deflection $w(L/2, 2\pi/2)$ values are increasing linearly with q_0 for all different values of R_n . The most rapid increasing of $w(L/2, 2\pi/2)$ with q_0 is occurred in the case of $R_n = 0.5$.

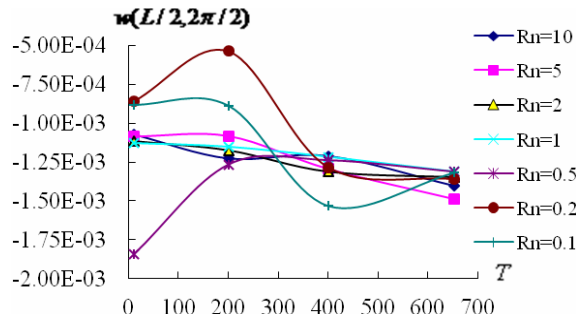


Fig. 7 $w(L/2, 2\pi/2)$ vs. T for $q_0 = 2 \text{ J}/(\text{s} \cdot \text{m}^2)$

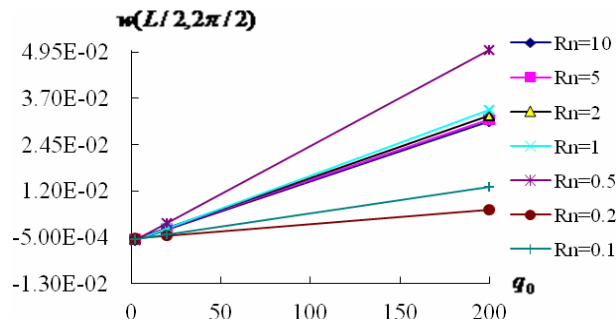


Fig. 8 $w(L/2, 2\pi/2)$ vs. q_0 for $T = 100^\circ \text{K}$

4. Conclusions

Deflections and stresses of thermal vibration results in the rapid heating of circular cylindrical Terfenol-D FGM shells with the FSĐT effect are obtained by using the GDQ method. The constant shear correction factor used for the cases investigated in the present paper usually provide a referred data. In the future study, a corrected shear correction factor should be calculated for FGM, usually they are varied with thickness of plates, FGM power law index and environment temperature. The use of FSĐT model for Terfenol-D FGM shell is a big limitation for obtaining the linear, simple, preliminary and basic calculation results. Similarly thick shell problems in the further would be investigated with non-linear, refined and higher order models to get more accurate results.

References

1. Livshits M. and Kribus A., 'Solar hybrid steam injection gas turbine (STIG) cycle', *Solar Energy*, **86** (2012), 190–199.
2. Li X.P., Gong N.N., Guan Y.J. and Cheng G.M., 'Thermal and stress analysis of rapid electric heating injection mold for a large LCD TV panel', *App. Thermal Eng.*, **31** (2011), 3989–3995.
3. Bahtui A. and Eslami M.R., 'Coupled thermoelasticity of functionally graded cylindrical shells', *Mech. Research Comm.*, **34** (2007), 1–18.
4. Ponnusamy P. and Selvamani R., 'Wave propagation in a transversely isotropic magneto thermo elastic cylindrical panel', *Euro. J. of Mech. - A/Solids*, **39** (2013), 76–85.
5. Qatu M.S., Sullivan R.W. and Wang W., 'Recent research advances on the dynamic analysis of composite shells: 2000–2009', *Comp. Structure*, **93** (2010), 14–31.

6. Lee S.J., Reddy J.N. and Rostam-Abadi F., 'Nonlinear finite element analysis of laminated composite shells with actuating layers', *Fin. Elem. in Anal. & Design*, **43** (2006), 1–21.
7. Jafari A.A., Khalili S.M.R. and Azarafza R., 'Transient dynamic response of composite circular cylindrical shells under radial impulse load and axial compressive loads', *Thin-Walled Structure*, **43** (2005), 1763–1786.
8. Hong C.C., 'Thermal vibration and transient response of magnetostrictive functionally graded material plates', *Euro. J. of Mech. -A/Solids*, **43** (2014), 78–88.
9. Hong C.C., 'Thermal vibration of magnetostrictive functionally graded material shells', *Euro. J. of Mech.-A/Solids*, **40** (2013), 114–122.
10. Hong C.C., 'Computational approach of piezoelectric shells by the GDQ method', *Comp. Structure*, **92** (2010), 811–816.
11. Chi S.H. and Chung Y.L., 'Mechanical behavior of functionally graded material plates under transverse load, Part I: Analysis', *Int. J. of Solids and Structure*, **43** (2006), 3657–3674.
12. Bert C.W., Jang S.K. and Striz A.G., 'Nonlinear bending analysis of orthotropic rectangular plates by the method of differential quadrature', *Comp. Mech.*, **5** (1989), 217–226.
13. Shu C. and Du H., 'Implementation of clamped and simply supported boundary conditions in the GDQ free vibration analyses of beams and plates', *Int. J. Solids and Structure*, **34** (1997), 819–835.
14. Lee S.J. and Reddy J.N., 'Non-linear response of laminated composite plates under thermomechanical loading', *Int. J. of Non-linear Mech.*, **40** (2005), 971–985.
15. Hetnarski R.B., *Thermal Stresses II*, Elsevier Science Publishers B.V., 1987, 332–336.
16. Carslaw H.S. and Jaeger J.C., *Conduction of Heat in Solids*, Oxford University Press, London, 1959.
17. Hong C.C., 'Rapid heating induced vibration of circular cylindrical shells with magnetostrictive functionally graded material', *Archives of Civil and Mech. Eng.*, **14** (2014), 710–720.
18. Reddy J.N. and Chin C.D., 'Thermoelastical analysis of functionally graded cylinders and plate', *J. Therm. Stress*, **21** (1998), 593–626.
19. Shariyat M., 'Dynamic buckling of suddenly loaded imperfect hybrid FGM cylindrical shells with temperature dependent material properties under thermo-electromechanical loads', *J. of Mech. Sci.*, **50** (2008), 1561–1571.
20. Hong C.C., 'Thermal vibration of magnetostrictive functionally graded material shells by considering the varied effects of shear correction coefficient', *Int. J. of Mech. Sci.*, **85** (2014), 20–29.